

# Alloy catalysts designed from first principles

JEFF GREELEY AND MANOS MAVRIKAKIS\*

Department of Chemical and Biological Engineering, University of Wisconsin-Madison, Madison, Wisconsin 53706, USA

\*e-mail: manos@engr.wisc.edu

Published online: 17 October 2004; doi:10.1038/nmat1223

The rational design of pure and alloy metal catalysts from fundamental principles has the potential to yield catalysts of greatly improved activity and selectivity. A promising area of research concerns the role that near-surface alloys (NSAs) can play in endowing surfaces with novel catalytic properties. NSAs are defined as alloys wherein a solute metal is present near the surface of a host metal in concentrations different from the bulk; here we use density functional theory calculations to introduce a new class of these alloys that can yield superior catalytic behaviour for hydrogen-related reactions. Some of these NSAs bind atomic hydrogen (H) as weakly as the noble metals (Cu, Au) while, at the same time, dissociating H<sub>2</sub> much more easily. This unique set of properties may permit these alloys to serve as low-temperature, highly selective catalysts for pharmaceuticals production and as robust fuel-cell anodes.

Rational catalyst design has long been a goal of surface scientists and engineers<sup>1,2</sup>, and recent investigations have begun to elucidate some of the principles necessary for such efforts to be successful<sup>3-6</sup>. NSAs, in particular, have shown promise for catalyst design<sup>3,7,8</sup>, and single-crystal investigations have demonstrated some of their remarkable properties in a limited number of cases. For example, thin layers of platinum on Ru(0001) crystals greatly reduce the strength of CO binding compared with pure Pt(111) surfaces<sup>9</sup>. Similarly, a small amount of nickel dosed on Pt(111) significantly decreases the desorption temperature of hydrogen compared with the respective pure metal surfaces<sup>10</sup>. Finally, vapour-deposited vanadium aids CO hydrogenation on Pd(111) and Rh(111)<sup>11</sup>.

Hydrogen chemistry on NSAs is of particular interest, as this element has so important a role in many chemical<sup>12,13</sup> and pharmaceutical<sup>14</sup> processes. Hydrogen is also increasingly used in energy production and storage technologies<sup>15-19</sup>, including fuel cells. To develop new NSAs for such processes, we use periodic, self-consistent density functional theory calculations that have shown considerable predictive power for catalysis<sup>20</sup>. Using simple models, we evaluate the stability of a large class of NSAs in hydrogen-rich environments, and we discuss the reactivity of hydrogen on the resulting stable surfaces. We find, among other results, that some NSAs produce a combination of weak hydrogen binding and easy H<sub>2</sub> dissociation. These unusual characteristics could be beneficial both for H<sub>2</sub> dissociation to produce adsorbed H and for subsequent reactions of H with other surface species. For H<sub>2</sub> dissociation, weak binding of H would generally be thought to imply a high H<sub>2</sub> activation energy barrier<sup>21-23</sup>. We find, however, that selected NSAs offer an exciting exception to this rule by simultaneously allowing weak H binding and low H<sub>2</sub> dissociation barriers. Weak binding of H, in turn, can make subsequent reaction steps easier, thereby allowing lower temperatures to be used for reactions on these NSAs.

We begin by describing how NSAs for hydrogen-related reactions can be chosen. Initially, we focus on two idealized classes of these alloys; in both cases, a total solute coverage of one monolayer in the near-surface region is assumed. Later, we discuss the effects of deviations from these idealized cases. To identify NSAs with well-defined properties, it is desirable that the composition in the near-surface region be stable in hydrogen-rich environments at appropriate temperatures and pressures. The stability can be assessed using a simple, two-step procedure, first considering the composition in vacuum, and then accounting for the effects of hydrogen adsorption.

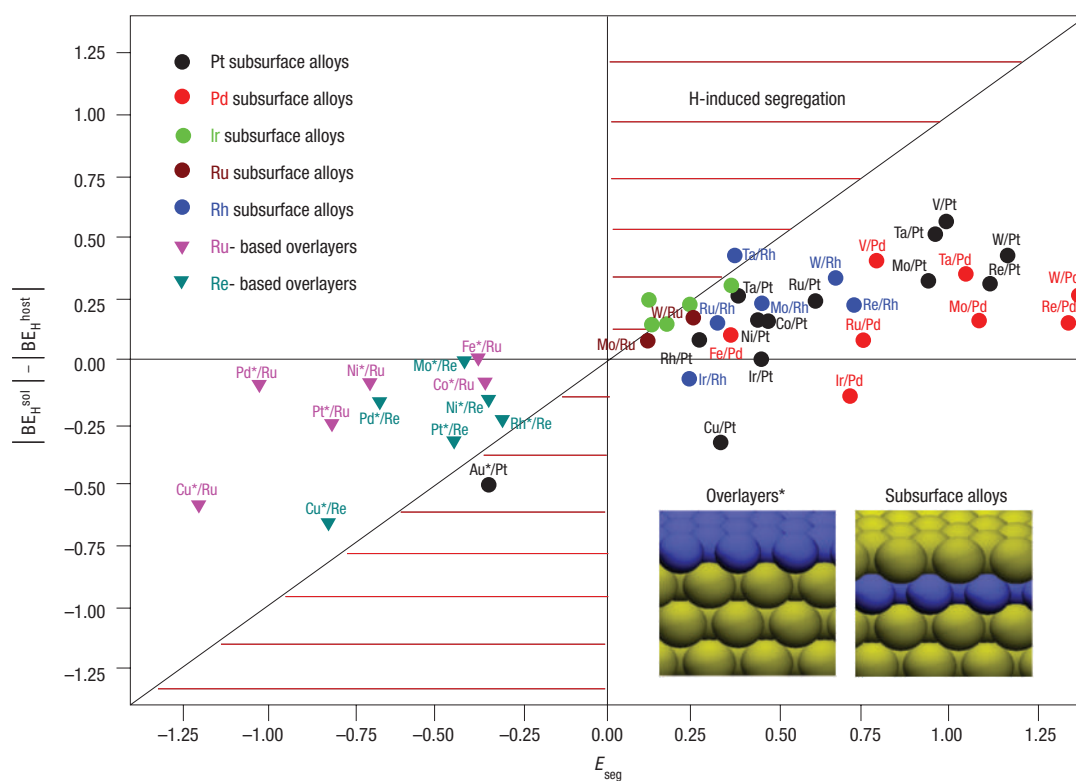


**Figure 1** Stability of NSAs with respect to hydrogen-induced segregation. Metal alloys are denoted as solute/host pairs. The x axis indicates the energy ( $E_{\text{seg}}$ ) for a single solute atom to move from the bulk to the surface layer of the host metal. The y axis denotes the difference between the magnitudes of the hydrogen binding energies ( $\theta_{\text{H}} = 1/4$  monolayer) on the pure solute ( $|BE_{\text{H}}^{\text{sol}}|$ ) and on the pure host ( $|BE_{\text{H}}^{\text{host}}|$ ) close-packed metal surfaces. Regions in which hydrogen-induced segregation is expected are hatched. The \* symbol denotes overlayers; otherwise, subsurface alloys (see inset schematics) are present. See text in connection to the Au\*/Pt system. The colour code used for each class of NSAs, characterizing the host metal used for the class, is preserved in subsequent figures.

The first step is to estimate the surface composition in vacuum from the solute/host segregation energy database of Ruban *et al.*<sup>24</sup>. The segregation energy ( $E_{\text{seg}}$ ) is the energy required to move a solute atom from the bulk to the surface of the host metal. If this energy is sufficiently negative, the surface layer will be pure solute, and an overlayer structure will result (Fig. 1 inset); if it is sufficiently positive, the surface layer will be pure host (we have found that, within the context of our surface model, even small segregation energies are enough to ensure that the surface layer on a close-packed surface will be a pure metal; see Supplementary Information, Table S1). In the latter case, solute deposited on the surface of the host metal preferentially segregates to the subsurface metal layer (high-temperature annealing may be required to overcome kinetic barriers for this process to occur) and a subsurface alloy forms (Fig. 1 inset), as a few groups have observed experimentally<sup>10,25,26</sup>.

The second step in determining the stability of NSAs is to assess the effect of hydrogen adsorption on the surface composition. In general, adsorbates can draw to the surface components of alloys to which they bind strongly. We have found, for example, that the thermodynamics are favourable for hydrogen to pull substrate Pt atoms to the Au surface of the Au\*/Pt overlayer NSA. Such effects complicate modelling efforts, and we have therefore focused our attention on cases where there is no significant adsorbate-induced segregation. We find that a reliable estimate of the tendency of hydrogen to induce surface segregation can be made by comparing  $E_{\text{seg}}$  of the solute to the difference in the magnitudes of the hydrogen binding energies between the pure solute and the pure host

( $|BE_{\text{H}}^{\text{sol}}| - |BE_{\text{H}}^{\text{host}}|$ , where  $BE_{\text{H}}$  is the energy change when atomic hydrogen is adsorbed from the gas phase onto the metal surface; see Fig. 1). If, for example,  $E_{\text{seg}}$  is positive, then in vacuum the solute will be found in the subsurface layers of the host. Further, if H binds more strongly to the host than to the solute, surface hydrogen will not attract the solute to the surface, and no hydrogen-induced segregation will occur. Hence, there is no H-induced segregation for the few solute/host pairs that lie in the lower right and upper left quadrants of Fig. 1. In the upper right and lower left quadrants, the parity line divides segregating from non-segregating regions. We have confirmed that this simple technique reliably predicts segregation behaviour in the presence of hydrogen, although there may be exceptions in cases where  $E_{\text{seg}}$  and  $|BE_{\text{H}}^{\text{sol}}| - |BE_{\text{H}}^{\text{host}}|$  are within  $\sim 0.1$  eV of one another (see Supplementary Information, Table S2). In general, Fig. 1 suggests that hydrogen will not induce surface segregation for most solute/host transition metal pairs, at least at low temperatures and pressures. This analysis can be extended to estimate the stability of NSAs in more complicated, multi-adsorbate reaction environments. The range of BEs of oxygen, sulphur and CO across the pure transition metals is larger than is the corresponding range for hydrogen (the range of BE between Au and Ru, for example, is 0.75 eV for H, 1.87 eV for CO, 2.25 eV for S and 2.70 eV for O), so these species will generally have larger thermodynamic driving forces for adsorbate-induced segregation.

A careful analysis of NSA structures and compositions with the above ‘screening’ approach based on first principles should allow physically meaningful NSA configurations to be identified.

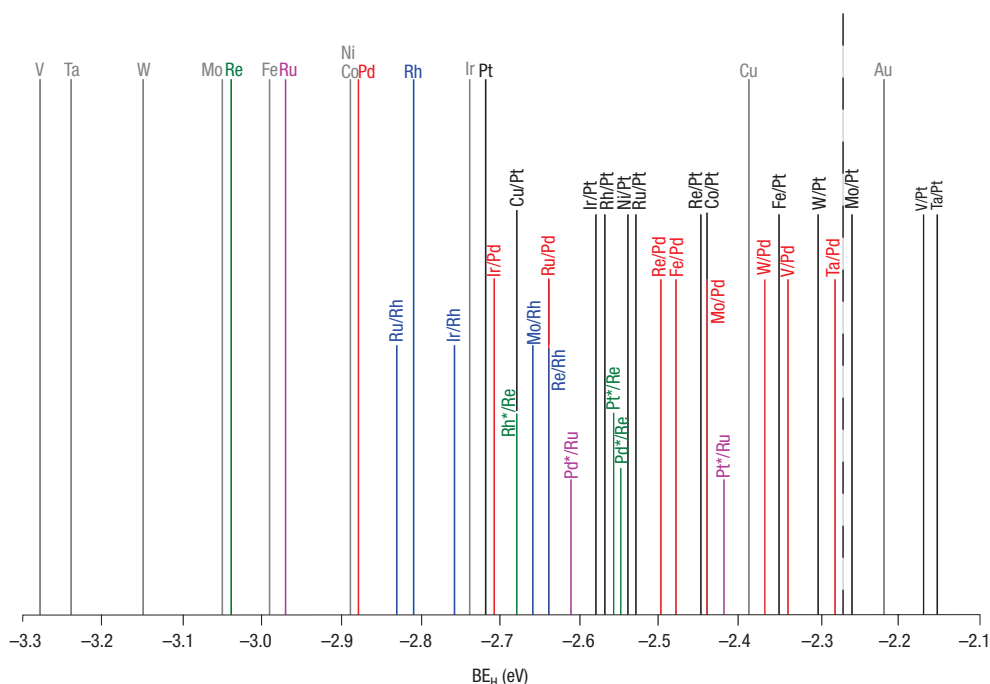


**Figure 2** Hydrogen binding energies ( $BE_H$ ) on various close-packed surfaces. Referenced to a clean metal slab and a gas-phase hydrogen atom ( $H(g)$ ) at infinite separation from one another. The height of the bars associated with the various alloys and pure metals is arbitrary and is varied only for clarity. The vertical dashed line at  $-2.28$  eV corresponds to thermoneutral  $H_2(g)$  dissociation (the gas-phase  $H_2$  bond energy is  $4.57$  eV).

Real NSAs may, nonetheless, differ in certain ways from our idealized NSA models. In some cases, a portion of the solute in a subsurface alloy may segregate more deeply into the host. For example, on a five-layer W/Pt(111) subsurface alloy (a system with a very positive segregation energy), it is energetically favourable for two out of four W atoms (total W coverage = 1 monolayer) to segregate to the third metal layer, leaving only two in the second layer. In other cases, the total coverage of solute in the surface region may differ from one monolayer, leading to different types of subsurface alloy structures<sup>26</sup>. In still other situations, arrangements of atoms with unusual periodicity (or even no periodicity at all) may permit the formation of defects or long-range reconstructions<sup>27,28</sup> (see Supplementary Information, Note 1). We have found that these possible deviations from our idealized NSA structures do not substantially affect the main trends in adsorbate behaviour presented below (some experimental studies have already shown significantly modified catalytic activity, along the lines of our theoretical predictions, even on non-ideal NSAs<sup>10,11</sup>). However, the deviations from the idealized cases do have a quantitative effect on the properties of adsorbates on these NSAs. Thus, to benefit fully from the unique catalytic properties of NSAs, more precise control of metal catalyst surface structure will be needed, perhaps through improved nanofabrication techniques. Recent innovations in atomic layer deposition and in nanoparticle fabrication technologies for metals suggest that practical nanofabrication strategies for metals may not be far off<sup>29–31</sup>.

We now describe the properties of hydrogen on stable, ideal NSAs. Figure 2 gives the hydrogen binding energy on the close-packed surfaces of a wide variety of pure metals and NSAs (see Supplementary Information Note 2, for a discussion of other crystal facets, and Table S3 for binding-energy values). The range of  $BE_H$ s across all pure metals studied ( $\sim 1.1$  eV) reflects a broad spectrum

of catalytic activities for hydrogen-based processes. The figure also demonstrates that NSAs generally bind hydrogen more weakly than do pure metals. The only pure metals with lower  $|BE_H|$  than platinum are the noble metals (Cu, Au). Many NSAs, however, have  $BE_H$ s in this range, generating a quasi-continuous spectrum of binding energies. In fact, certain of the subsurface alloys (for example, with the hosts Pt or Pd, and solutes Ta, W or V) bind hydrogen more weakly than do pure Cu and/or Au. Migration of solute atoms deeper into these subsurface alloys does reduce the calculated decrease in  $|BE_H|$  compared with the pure host, but the decrease is still significant (the migration of two W atoms to the third metal layer, described above, cancels only  $\sim 25\%$  of the  $|BE_H|$  decrease found in the W/Pt ideal subsurface alloy where all W atoms are in the second layer; see also Supplementary Information, Note 3). Furthermore, weaker binding of surface hydrogen does not imply weaker binding of subsurface hydrogen. For most of the Pt subsurface alloys studied in this work, the energy difference between surface and subsurface H is lowered compared with pure Pt (for example, this difference is  $0.68$  eV for pure Pt and  $0.47$  eV for Co/Pt subsurface alloys). This property points to potential applications of NSAs for hydrogen separation and storage.

To rationalize the variation in  $BE_H$  shown in Fig. 2, we present two correlations between  $BE_H$  and properties of the clean alloy surfaces (Fig. 3; see also Table S4 in Supplementary Information). The first involves relating  $BE_H$  to the  $d$ -band centre,  $\epsilon_d$  (ref. 32), of the NSAs (Fig. 3a). The closer the  $\epsilon_d$  is to the Fermi level, the stronger the hydrogen binding is; differences between the best-fit lines of the correlation for subsurface alloys with different hosts are mainly due to the differing coupling matrix elements of the respective hosts<sup>20,33</sup>. The scatter in the correlation is probably caused by the small size of the atomic H orbitals, leading to a relatively weak coupling between

H and the  $d$  orbitals. The second correlation involves relating  $\Delta(\text{BE}_{\text{H}})$  to  $\Delta E_{\text{su}}$ . The quantity  $\Delta(\text{BE}_{\text{H}})$  is the difference between  $\text{BE}_{\text{H}}$  on the pure host or solute metal (depending on which metal is in the surface layer of the alloy) and on the NSA, and  $\Delta E_{\text{su}}$  is the corresponding difference between the BEs of the surface metal layer (Fig. 3b). With a V(solute)/Pd(host) subsurface alloy, for example,  $\Delta(\text{BE}_{\text{H}})$  is the difference between  $\text{BE}_{\text{H}}$  on pure Pd(111) and on the V/Pd(111) NSA, and  $\Delta E_{\text{su}}$  is the difference between the binding energy of the top Pd layer on pure Pd(111) and that of the top Pd layer on the NSA (per surface metal atom). Although the detailed physics behind the relationship of  $\Delta(\text{BE}_{\text{H}})$  to  $\Delta E_{\text{su}}$  is complex, the trend can be qualitatively understood as follows: if the surface metal layer is an electron-rich metal (for example, Pt or Pd), then this layer couples to any electron-poor elements in the subsurface layer (for example, Ta, W or V), thereby leading to a strong metal–metal interlayer bond. The strengthening of this bond, in turn, weakens the bonding of the surface layer to the adsorbate<sup>34</sup>.

The low dissociation barrier of  $\text{H}_2$  on NSAs is the most promising property of these materials for hydrogen-related catalytic applications. Hydrogen binds weakly to the noble metals (Fig. 2), and  $\text{H}_2$  dissociation is highly activated on those metals<sup>35</sup>. These facts might be taken to suggest that any alloy with  $\text{BE}_{\text{H}}$ s comparable to those of the noble metals will be inactive for  $\text{H}_2$  dissociation. Our results indicate, however, that the transition-state energies for  $\text{H}_2$  dissociation on Cu and Au are significantly higher than are the transition-state energies on NSAs with comparable  $\text{BE}_{\text{H}}$ s (Fig. 4). In fact, there is a distinct line correlating the transition-state energy with the atomic  $\text{BE}_{\text{H}}$  for each family of NSAs terminated with a given element. Two such families are shown in Fig. 4; one includes both subsurface alloys where Pd is the host and modestly strained Pd overlayers on other elements, whereas the other corresponds to Pt-terminated NSAs (the particular NSAs in each family were chosen because they have  $\text{BE}_{\text{H}}$ s comparable to those of the noble metals). The lowering of the transition-state energy is observed even on non-ideal NSAs although the effect is less pronounced. For example, on the non-ideal W/Pt alloy described above, the transition-state energy is found to be  $\sim 0.16$  eV, compared with  $\sim 0.18$  eV on the ideal W/Pt(111) subsurface alloy.

The above property is unique; according to similar correlations for a number of simple dissociation reactions<sup>21–23</sup>, weaker H binding should always imply a higher  $\text{H}_2$  dissociation barrier. Near-surface alloys, however, escape from that rule by offering the exciting combination of weak hydrogen binding and easy  $\text{H}_2$  activation. Here, we discuss the observed lowering of the transition-state energy from three different perspectives. First, we analyse the transition-state energies using the Hammer–Nørskov model<sup>33,36</sup> (see Supplementary Information, Note 4, Table S5 and Fig. S1); that model assumes that interactions between the  $\sigma_{\text{g}}$  (highest occupied) and  $\sigma_{\text{u}}$  (lowest unoccupied) molecular orbitals of  $\text{H}_2$  and the  $s, p$ -bands of the metal surfaces contribute a roughly constant amount of energy to the transition state for all metals; interactions with the metal  $d$ -bands are metal-dependent and are treated as perturbations to the  $s, p$  contributions. This treatment is highly approximate (for example, the width of the  $d$ -band is not explicitly accounted for), but it seems to be accurate enough to capture qualitative trends in the transition-state energies for geometrically similar transition-state structures. For the purpose of the Hammer–Nørskov analysis, therefore, we had to assume that the transition-state geometry for all systems examined (see Table S5) was identical; this assumption ignores the effect of detailed geometric structure on the transition-state energy. Analysis of the model results suggests that the extra stabilization of the transition state on the NSAs originates mainly from the interaction of the  $\sigma_{\text{u}}$  orbital with the  $d_{xz}$  and the  $d_{yz}$  metal states (the transition state lies on the diagonal of our unit cell), which is much stronger than the corresponding interaction on the

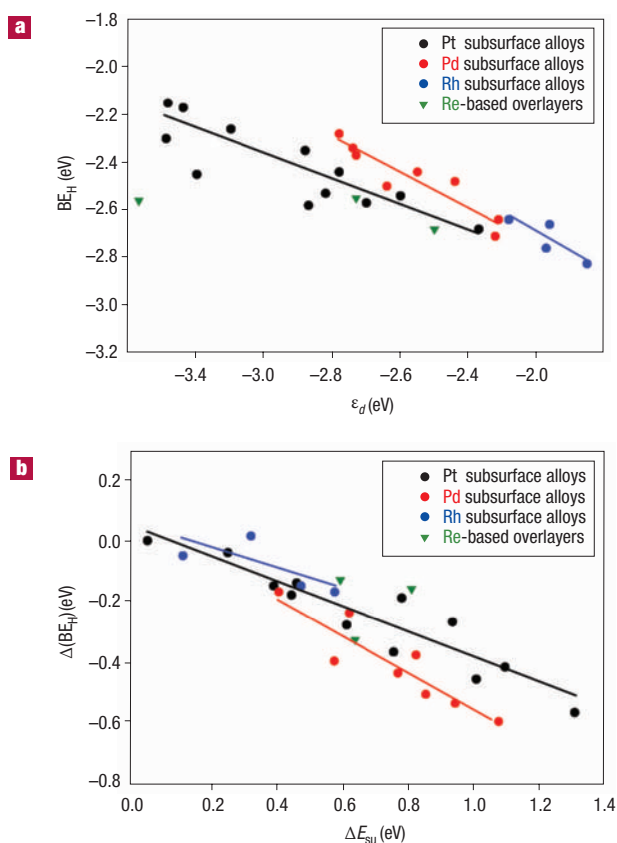


**Figure 3** Correlation of the binding energy of atomic hydrogen,  $\text{BE}_{\text{H}}$ , with properties of the clean NSA surfaces. **a**, Plot of  $\text{BE}_{\text{H}}$  (referenced as explained in Fig. 2) versus the  $d$ -band centre of the corresponding surface. Coloured lines are best fits for the classes of subsurface alloys of the same host. **b**, Plot of  $\Delta(\text{BE}_{\text{H}})$  versus  $\Delta E_{\text{su}}$ . The difference in binding energy  $\Delta(\text{BE}_{\text{H}}) = \text{BE}_{\text{H}}(\text{on pure metal corresponding to element in top layer of NSA}) - \text{BE}_{\text{H}}(\text{on NSA})$ . A negative  $\Delta(\text{BE}_{\text{H}})$  means that H binding is weaker on the NSA than on a pure slab of the terminating-element metal. The difference  $\Delta E_{\text{su}} = \text{BE}(\text{top layer of pure metal slab}) - \text{BE}(\text{top layer of NSA})$  (per surface atom basis). A positive  $\Delta E_{\text{su}}$  indicates stronger binding of the top metal layer in the NSA than in its own pure slab. Circles indicate subsurface alloys, and inverted triangles denote overlayers. See also Supplementary Information.

noble metals. Furthermore, compared with the noble metals, there is an additional stabilization to the transition state on the NSAs, due to the interaction of the  $\sigma_{\text{g}}$  orbital with the  $d_{z^2}$  metal states, but it is much smaller than the  $\sigma_{\text{u}}-d_{xz}/d_{yz}$  stabilization. Part of the transition-state stabilization observed in the NSAs may be the result of (1) geometric deviations from the common transition-state structure considered for the purpose of this analysis, and (2) a possibly decreased Pauli repulsion of the adsorbate orbitals with the  $s, p$  metal states, which is ignored in the Hammer–Nørskov model. A more detailed study of  $\text{H}_2$  dissociation on specific NSAs should be able to quantify the effect of these factors on the observed transition-state stabilization.

Second, we suggest that the unusually low transition-state energies on the NSAs might be analysed by looking at the reverse reaction (that is, the hydrogen association) barriers on these surfaces. The barriers are increased significantly on the noble metals by the energy cost needed to activate H atoms to the transition state. The Pd-terminated alloys have a comparable H activation cost, but

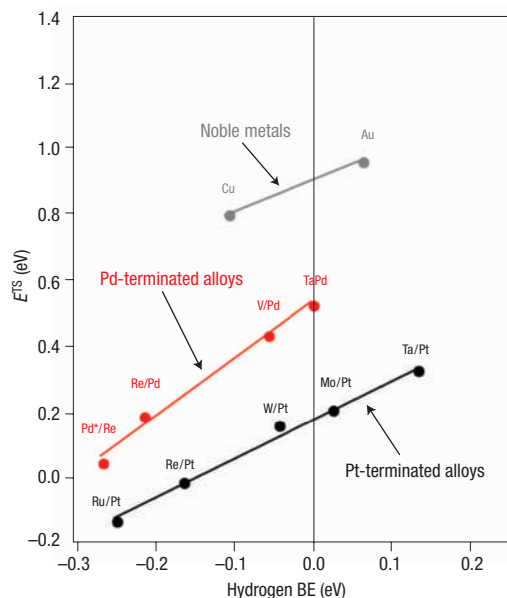


**Figure 4** Transition-state ( $E^{TS}$ ) energy versus hydrogen binding energy for  $H_2$  dissociation on pure noble metals and NSAs. In variance with previous figures, the energy reference for both  $E^{TS}$  and the hydrogen BE corresponds to  $H_2(g)$  and the clean metal slab at infinite separation from one another. Thus, the zero of the x axis corresponds to the dashed line of Fig. 2.

attraction between the two H atoms at the transition state stabilizes the saddle point. The Pt-terminated alloys, on the other hand, have very small H activation costs and modest attraction or repulsion at the transition states, leading to low transition-state energies and to low  $H_2$  desorption temperatures (as shown experimentally<sup>10</sup> for Ni/Pt(111)).

Finally, on NSAs, we find weakly bound molecular hydrogen precursors at top sites (test calculations have not shown significant entrance barriers for molecular hydrogen adsorption). Such precursor states do not exist on the noble metals, pointing to a different interaction between the  $H_2$  orbitals and the metal  $d$ -states; this modified interaction might also affect the transition-state energies. We note, in passing, that the existence of ‘on top’ precursors led us to focus primarily on over-top dissociation paths in our calculations (although we have found little difference in the barriers when checking other pathways; see elsewhere<sup>37</sup> for further discussion of the V/Pd(111) system). In general, although we have focused primarily on  $H_2$  dissociation in this study, we expect that similarly decreased transition-state energies might be found on NSAs for other reactions. We have determined, for example, that the transition state for methane activation ( $H_3C-H$  scission) on a Ta/Pt(111) subsurface alloy is  $\sim 0.5$  eV lower in energy than is the corresponding transition state on Au(111), although the products of this reaction have very similar binding energies on the two surfaces.

The above results demonstrate that many NSAs may have favourable hydrogen dissociation kinetics in spite of their relatively weak hydrogen binding. Accordingly, NSAs promise high hydrogenation activity at low temperatures. At such temperatures, there is generally insufficient thermal energy available to activate competitive reaction pathways that produce by-products, and so the overall reaction selectivity should be increased.

This new class of near-surface alloys could thus assist in highly selective hydrogenation reactions at low temperatures, of particular

interest for the production of chiral pharmaceutical compounds, and could, potentially, permit easier separation and storage of hydrogen. By following a similar procedure, stable NSAs could be designed that bind CO weakly. This property, combined with the facile hydrogen activation described above, could lead to improved anode catalysts for low-temperature fuel cells. In our analysis, we have focused primarily on two idealized classes of NSAs: subsurface alloys and overlayers. Our quantitative predictions will change for non-ideal NSAs, but test calculations, together with experimental studies on non-ideal NSAs<sup>11</sup>, suggest that the qualitative trends established here will persist in those cases. Finally, as techniques for nanoscale materials synthesis improve, we suggest that it will become feasible to prepare desired, quasi-ideal NSAs<sup>29–31</sup> reproducibly, resulting in the design and manufacture of an even wider variety of such materials for use in catalysis and other important technological applications.

## METHODS

The total-energy, periodic, density functional theory calculations are done self-consistently with ultrasoft pseudopotentials, slabs of four metal layers ( $2 \times 2$  unit cell), plane waves with kinetic energies up to 25 Ry, and 18  $k$ -points in the first Brillouin zone<sup>38</sup>. Exchange and correlation effects are described within the generalized gradient approximation of Perdew *et al.*<sup>39</sup>. Relaxation of  $H$ ,  $H_2$  and the top two metal layers is allowed. Convergence of  $BE_H$  with respect to the various calculational parameters is confirmed to within 0.1 eV. In all cases, we have restricted our attention to alloys that are found to be stable in the presence of hydrogen (see text and Supplementary Information), and we have tested all possible H adsorption configurations on the most stable crystal facets of the metals ((111) for f.c.c. metals, (0001) for h.c.p. metals and (110) for b.c.c. metals). Transition states for  $H_2$  dissociation are located with the ‘climbing image nudged elastic band’ algorithm<sup>40</sup>. Spin-polarization effects are tested for and included where appropriate. Zero-point energy effects are not included; such effects are found to change the hydrogen binding energies by  $<0.05$  eV. The calculated gas-phase  $H_2$  bond energy is 4.57 eV, in good agreement with the experimental value of 4.52 eV at 298 K (ref. 41).

Received 22 December 2003; accepted 1 August 2004; published 17 October 2004.

## References

- Somorjai, G. A. *Introduction to Surface Chemistry and Catalysis* (Wiley, New York, 1994).
- Chorkendorff, I. & Niemantsverdriet, J. W. *Concepts of Modern Catalysis and Kinetics* (Wiley, Weinheim, 2003).
- Besenbacher, F. *et al.* Design of a surface alloy catalyst for steam reforming. *Science* **279**, 1913–1915 (1998).
- Jacobsen, C. J. H. *et al.* Catalyst design by interpolation in the periodic table: bimetallic ammonia synthesis catalysts. *J. Am. Chem. Soc.* **123**, 8404–8405 (2001).
- Zambelli, T., Wintterlin, J., Trost, J. & Ertl, G. Identification of the ‘active sites’ of a surface-catalyzed reaction. *Science* **273**, 1688–1690 (1996).
- Xu, Z. *et al.* Size-dependent catalytic activity of supported metal-clusters. *Nature* **372**, 346–348 (1994).
- Sinfelt, J. H. *Bimetallic Catalysts: Discoveries, Concepts, and Applications* (Wiley, New York, 1983).
- Nielsen, L. P. *et al.* Initial growth of Au on Ni(110): surface alloying of immiscible metals. *Phys. Rev. Lett.* **71**, 754–757 (1993).
- Schlapka, A., Lischka, M., Groß, A., Käsberger, U. & Jakob, P. Surface strain versus substrate interaction in heteroepitaxial metal layers: Pt on Ru(0001). *Phys. Rev. Lett.* **91**, 016101 (2003).
- Hwu, H. H., Eng, J. Jr. & Chen, J. G. Ni/Pt(111) bimetallic surfaces: unique chemistry at monolayer Ni coverage. *J. Am. Chem. Soc.* **124**, 702–709 (2002).
- Klötzer, B., Unterberger, W. & Hayek, K. Adsorption and hydrogenation of CO on Pd(111) and Rh(111) modified by subsurface vanadium. *Surf. Sci.* **532–535**, 142–147 (2003).
- Hansen, P. L. *et al.* Atom-resolved imaging of dynamic shape changes in supported copper nanocrystals. *Science* **295**, 2053–2055 (2002).
- Mitsui, T., Rose, M. K., Fomin, E., Ogletree, D. F. & Salmeron, M. Dissociative hydrogen adsorption on palladium requires aggregates of three or more vacancies. *Nature* **422**, 705–707 (2003).
- Studer, M., Blaser, H. & Exner, C. Enantioselective hydrogenation using heterogeneous modified catalysts: an update. *Adv. Synth. Catal.* **345**, 45–65 (2003).
- Cortright, R. D., Davda, R. R. & Dumesic, J. A. Hydrogen from catalytic reforming of biomass-derived hydrocarbons in liquid water. *Nature* **418**, 964–967 (2002).
- Huber, G. W., Shabaker, J. W. & Dumesic, J. A. Raney Ni–Sn catalyst for  $H_2$  production from biomass-derived hydrocarbons. *Science* **300**, 2075–2077 (2003).
- Deluga, G. A., Salge, J. R., Schmidt, L. D. & Veyrakis, X. E. Renewable hydrogen from ethanol by autothermal reforming. *Science* **303**, 993–997 (2004).
- Turner, J. A. A realizable renewable energy future. *Science* **285**, 687–689 (1999).
- Schlapbach, L. & Züttel, A. Hydrogen-storage materials for mobile applications. *Nature* **414**, 353–358 (2001).
- Greeley, J., Norskov, J. K. & Mavrikakis, M. Electronic structure and catalysis on metal surfaces. *Ann. Rev. Phys. Chem.* **53**, 319–348 (2002).
- Norskov, J. K. *et al.* Universality in heterogeneous catalysis. *J. Catal.* **209**, 275 (2002).
- Xu, Y., Ruban, A. V. & Mavrikakis, M. The adsorption and dissociation of  $O_2$  on Pt–Co and Pt–Fe alloys. *J. Am. Chem. Soc.* **126**, 4717–4725 (2004).
- Michaelides, A. *et al.* Identification of general linear relationships between activation energies and enthalpy changes for dissociation reactions at surfaces. *J. Am. Chem. Soc.* **125**, 3704–3705 (2003).

24. Ruban, A. V., Skriver, H. L. & Nørskov, J. K. Surface segregation energies in transition-metal alloys. *Phys. Rev. B* **59**, 15990–16000 (1999).
25. Hugenschmidt, M. B., Ruff, M., Hitzke, A. & Behm, R. J. Rotational epitaxy vs. missing row reconstruction: Au/Cu/Au(110). *Surf. Sci.* **388**, L1100–L1106 (1997).
26. Konvicka, C. *et al.* Surface and subsurface alloy formation of vanadium on Pd(111). *Surf. Sci.* **463**, 199–210 (2000).
27. Okada, M., Nakamura, M., Moritani, K. & Kasai, T. Dissociative adsorption of hydrogen on thin Au films grown on Ir(111). *Surface Science* **523**, 218–230 (2003).
28. Lundgren, E., Leonardelli, G., Schmid, M. & Varga, P. A misfit structure in the Co/Pt(111) system studied by scanning tunnelling microscopy and embedded atom method calculations. *Surf. Sci.* **498**, 257–265 (2002).
29. Lim, B. S., Rahtu, A. & Gordon, R. G. Atomic layer deposition of transition metals. *Nature Mater.* **2**, 749–754 (2003).
30. Finke, R. G. in *Metal Nanoparticles: Synthesis, Characterization, and Applications* (eds Feldheim, D. L. & Foss, C. A. Jr) 17–54 (Marcel Dekker, New York, 2002).
31. Debe, M. in *Handbook of Fuel Cells-Fundamentals, Technology, and Applications* (eds Vielstich, W., Lamm, A. & Gasteiger, H. A.) 576–589 (Wiley, New York, 2003).
32. Mavrikakis, M., Hammer, B. & Nørskov, J. K. Effect of strain on the reactivity of metal surfaces. *Phys. Rev. Lett.* **81**, 2819–2822 (1998).
33. Hammer, B. & Nørskov, J. K. in *Chemisorption and Reactivity on Supported Clusters and Thin Films* (eds Lambert, R. M. & Pacchioni, G.) 285–351 (Kluwer, Netherlands, 1997).
34. Rodriguez, J. A. & Goodman, D. W. The nature of the metal–metal bond in bimetallic surfaces. *Science* **257**, 897–903 (1992).
35. Hammer, B. & Nørskov, J. K. Why gold is the noblest of all metals. *Nature* **376**, 238–240 (1995).
36. Hammer, B. & Nørskov, J. K. Electronic factors determining the reactivity of metal surfaces. *Surf. Sci.* **343**, 211–220 (1995).
37. Beutl, M. *et al.* There is a true precursor for hydrogen adsorption after all: the system H<sub>2</sub>/Pd(111) + subsurface V. *Chem. Phys. Lett.* **342**, 473–478 (2001).
38. Hammer, B., Hansen, L. B. & Nørskov, J. K. Improved adsorption energetics within density-functional theory using revised Perdew–Burke–Ernzerhof functionals. *Phys. Rev. B* **59**, 7413–7421 (1999).
39. Perdew, J. P. *et al.* Atoms, molecules, solids, and surfaces: applications of the generalized gradient approximation for exchange and correlation. *Phys. Rev. B* **46**, 6671–6687 (1992).
40. Henkelman, G., Uberuaga, B. P. & Jónsson, H. A climbing image nudged elastic band method for finding saddle points and minimum energy paths. *J. Chem. Phys.* **113**, 9901–9904 (2000).
41. *CRC Handbook of Chemistry and Physics* (CRC, New York, 1996).

#### Acknowledgements

NSF supported this work through a pre-doctoral fellowship (J.G.) and a CAREER award (M.M.). Additional partial support was provided by a DOE-BES Catalysis Science Grant. Calculations were made on DOE-NERSC, NPACI and MSCF-PNNL resources. We thank A. Gokhale, M.-S. Han, A. Nilekar and Y. Xu for their help, and F. Besenbacher, J. Chen, J. Dumesic and J. Nørskov for discussions.

Correspondence and requests for materials should be addressed to M.M. Supplementary Information accompanies the paper on [www.nature.com/naturematerials](http://www.nature.com/naturematerials)

#### Competing financial interests

The authors declare that they have no competing financial interests.